

Spin Photocurrents in Quantum Wells review part II, (part I: cond-mat/0304266)

Sergey D. Ganichev and Wilhelm Prettl

Fakultät für Physik, Universität Regensburg, 93040 Regensburg, Germany,

ABSTRACT

Spin photocurrents generated by homogeneous optical excitation with circularly polarized radiation in quantum wells (QWs) are reviewed. The absorption of circularly polarized light results in optical spin orientation due to the transfer of the angular momentum of photons to electrons of a two-dimensional electron gas (2DEG). It is shown that in quantum wells belonging to one of the gyrotrropic crystal classes a non-equilibrium spin polarization of uniformly distributed electrons causes a directed motion of electron in the plane of the QW. A characteristic feature of this electric current, which occurs in unbiased samples, is that it reverses its direction upon changing the radiation helicity from left-handed to right-handed and vice versa.

Two microscopic mechanisms are responsible for the occurrence of an electric current linked to a uniform spin polarization in a QW: the spin polarization induced circular photogalvanic effect and the spin-galvanic effect. In both effects the current flow is driven by an asymmetric distribution of spin polarized carriers in \mathbf{k} -space of systems with lifted spin degeneracy due to \mathbf{k} -linear terms in the Hamiltonian. Spin photocurrents provide methods to investigate spin relaxation and to conclude on the in-plane symmetry of QWs. The effect can also be utilized to develop fast detectors to determine the degree of circular polarization of a radiation beam. Furthermore spin photocurrents at infrared excitation were used to demonstrate and investigate monopolar spin orientation of free carriers.

Contents

4.2	Spin-galvanic effect	28
4.2.1	Spin galvanic effect in the presence of external magnetic field	28
4.2.2	Spin-galvanic effect at optical excitation without external fields	31
4.3	Monopolar spin orientation	33
4.3.1	Direct transitions between size-quantized subbands	33
4.3.2	Drude absorption due to indirect intra-subband transitions	34
4.4	Spin controlled nonlinearity of spin orientation induced CPGE	35
5	Spin-independent photocurrents at homogeneous excitation	36
5.1	Linear photogalvanic effect	38
5.2	Photon drag effect	39
6	Spin photocurrents caused by inhomogeneities	41
7	Summary	42
	Acknowledgement	43
	References	43

4.2 Spin-galvanic effect

4.2.1 Spin galvanic effect in the presence of external magnetic field

The spin photocurrent due to the spin-galvanic effect has been experimentally investigated by the method described in section 2.3.5 and depicted in Fig. 7 [29, 30, 40, 41]. A homogeneous non-equilibrium spin polarization perpendicular to the plane of (001)-grown QWs has been prepared by absorption of circularly polarized radiation at normal incidence. The measurements were carried out on *n*-type GaAs and InAs samples. In this experimental configuration the spin polarization does not yield an electric current. However, applying an in-plane magnetic field a spin-galvanic current has been observed in *n*-type materials for both visible and infrared radiation (Figs. 16-20).

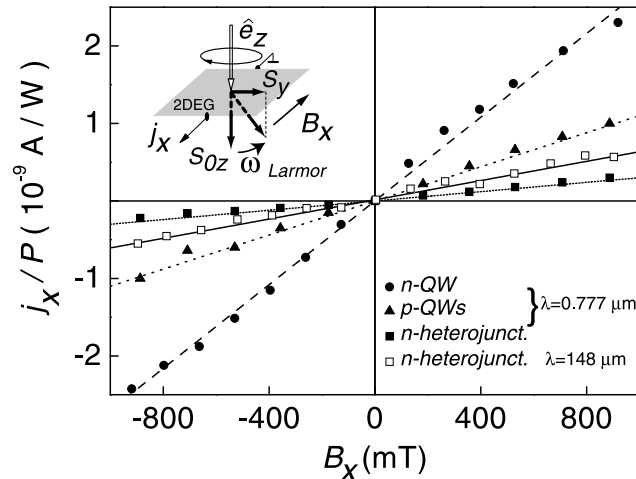


Figure 16: Spin-galvanic current j_x normalized by P as a function of magnetic field B for normally incident circularly polarized radiation at room temperature for various samples and wavelengths. Full symbols: $\lambda = 0.777 \mu\text{m}$, $P = 100 \text{ mW}$. Triangles, squares and circles correspond to *n*-type and *p*-type multiple QWs, and an *n*-type GaAs/AlGaAs heterojunction, respectively. Open squares: *n*-type GaAs/AlGaAs heterojunction, $\lambda = 148 \mu\text{m}$, $P = 20 \text{ kW}$. The inset shows the geometry of the experiment where \hat{e}_z indicates the direction of the incoming light.

For low magnetic fields B where $\omega_L \tau_s < 1$ holds, the photocurrent increases linearly as expected from Eqs. (25) and (30). This is seen in the room temperature data of Figs. 16 and 17 as well as in the 4.2 K data in Fig. 18 for $B \leq 1 \text{ T}$. The polarity of the current depends on the direction of the excited spins (see Figs. 17 and 18, $\pm z$ -direction for right or left circularly polarized light, respectively) and on the direction of the applied magnetic field (see Figs. 16-19, $\pm B_x$ -direction). For magnetic field applied along $\langle 110 \rangle$ the current is parallel (anti-parallel) to the magnetic field vector. For $B \parallel \langle 100 \rangle$ both the transverse and the longitudinal effects are observed [30]. This observation as well as helicity dependence of the photocurrent current shown in Fig. 19 are in good agreement to the phenomenological relation (see Eqs. (32)).

Comparing the power sensitivity for visible and infrared excitation we find them to be of the same order of magnitude as seen in Fig. 16. However, we note that the current contribution *per photon* is by two orders of magnitude larger for inter-band excitation compared to intra-subband absorption. This is due to a more effective spin generation rate by inter-band transitions. It may be even larger since the current gets partially shortened by photogenerated carriers in the semi-insulating substrate. For higher magnetic fields the current assumes a maximum and decreases upon further increase of B , as shown in Fig. 18. This drop of the current is ascribed to the Hanle effect [3]. The experimental data are well described by Eqs. (25) and (30). The observation of the Hanle effect demonstrates that free carrier intra-subband transitions can polarize the spins of electron systems. The measurements allow to obtain the spin relaxation time τ_s from the peak position of the photocurrent where $\omega_L \tau_s = 1$ holds [29].

In *p*-GaAs QWs at infrared excitation causing spin polarization of holes only, no spin-galvanic effect could be detected [29, 30]. In contrast to infrared experiments a current signal has been

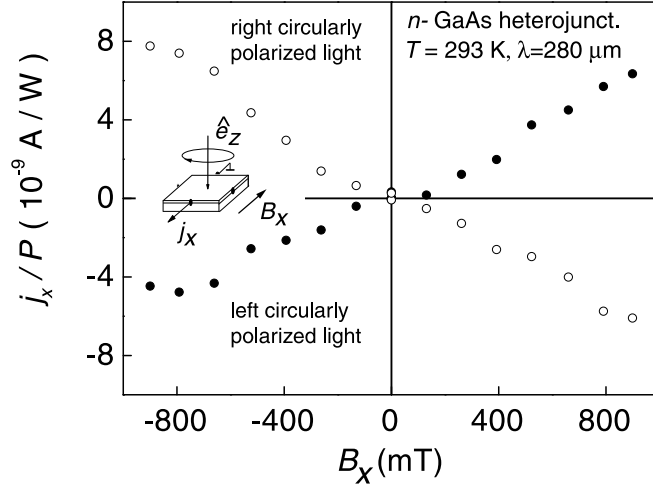


Figure 17: Magnetic field dependence of the spin-galvanic current normalized by P achieved by intra-subband transitions within $e1$ conduction subband by excitation with radiation of $\lambda = 280 \mu\text{m}$ wavelength. Results are plotted for an (001)-grown GaAs single heterojunction at room temperature.

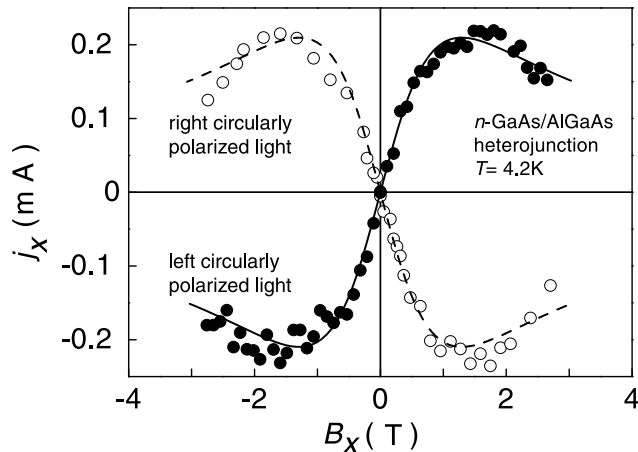


Figure 18: Spin-galvanic current j_x as a function of magnetic field B for normally incident right-handed (open circles) and left-handed (solid circles) circularly polarized radiation at $\lambda = 148 \mu\text{m}$ and radiation power 20 kW. Measurements are presented for an n -type GaAs/AlGaAs single heterojunction at $T = 4.2 \text{ K}$. Solid and dashed curves are fitted after Eqs. (25) and (30) using the same value of the spin relaxation time τ_s and scaling of the ordinate.

detected in *p*-type samples for visible excitation which polarize both electrons and holes (see Fig. 16). This current is due to the spin polarization of electrons only, which are in this case the minority carriers generated by inter-band excitation. The spin-galvanic effect in *p*-type material at inter- or intra-subband excitation could not be observed because of the experimental procedure which makes use of the Larmor precession to obtain an in-plane spin polarization. It is due to the fact that the in-plane *g*-factor for heavy holes is very small [108] which makes the effect of the magnetic field negligible [29]. This result does not exclude the spin-galvanic effect in *p*-type materials which might be observable by hole injection with spins in the plane of the QW.

Spin photocurrents due to the spin-galvanic effect have been recorded for inter-band, inter-subband, as well as for intra-subband transitions [29–31].

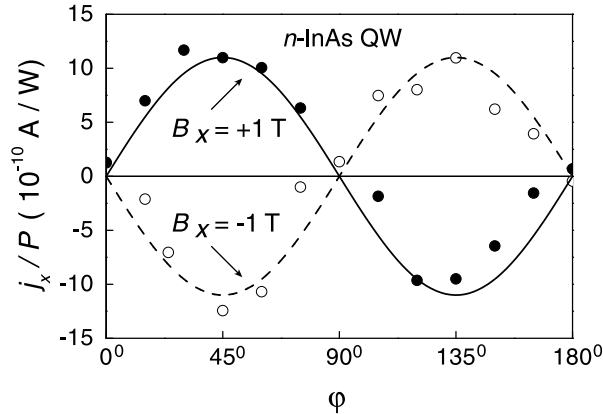


Figure 19: Spin-galvanic current normalized by P as a function of the phase angle φ in an (001)-grown *n*-type InAs QW of 15 nm width at $T = 4.2$ K. The photocurrent excited by normal incident radiation of $\lambda = 148$ μm is measured in x -direction parallel (full circles) and anti-parallel (open circles) to the in-plane magnetic field B_x . Solid and dashed curves are fitted after Eqs. (32) using the same scaling of the ordinate.

Inter-band transitions have been investigated in *n*- and *p*-type GaAs using circularly polarized light of a Ti:sapphire laser at $\lambda = 0.777$ μm . In this experiment electrons are excited from the valence band to the conduction band yielding a spin polarization in the conduction band due to selection rules.

Direct inter-subband transitions have been achieved in GaAs QWs of 8.2 nm and 8.6 nm widths at absorption of radiation in the range of 9 μm to 11 μm wavelength [40,41]. Applying MIR radiation of the CO₂ laser the spin-galvanic current at normal incidence of radiation has been observed. In contrast to spin orientation induced CPGE the wavelength dependence of the spin-galvanic effect obtained between 9.2 μm and 10.6 μm repeats the spectral behaviour of direct inter-subband absorption (see Fig. 20). This observation is in agreement with the mechanism of the spin-galvanic effect and the microscopic theory presented in section 2.3.3. The occurrence of a spin-galvanic current requires only a spin polarization in the lower subband and asymmetric spin relaxation. In the present case the spin orientation is generated by resonant spin-selective optical excitation followed by spin-non-specific thermalization. Therefore the magnitude of the spin polarization and hence the current depends on the absorption strength but not on the momentum \mathbf{k} of optical transition as in the case of CPGE described in section 2.2.1.

We would like to emphasize that spin sensitive $e1\text{-}e2$ inter-subband transitions in *n*-type QWs have been observed at normal incidence when there is no component of the electric field of the radiation normal to the plane of the QWs. Generally it is believed that inter-subband transitions in *n*-type QWs can only be excited by infrared light polarized in the growth direction z of the QWs [14]. Furthermore such transitions are spin insensitive and, hence, do not lead to optical orientation. Since the argument, leading to these selection rules, is based on the effective mass approximation in a single band model, the selection rules are not rigorous. The mechanism which leads to spin orientation in this geometry will be discussed in the section 4.3.1.

At indirect transitions the spin-galvanic effect as in the case of spin orientation induced CPGE

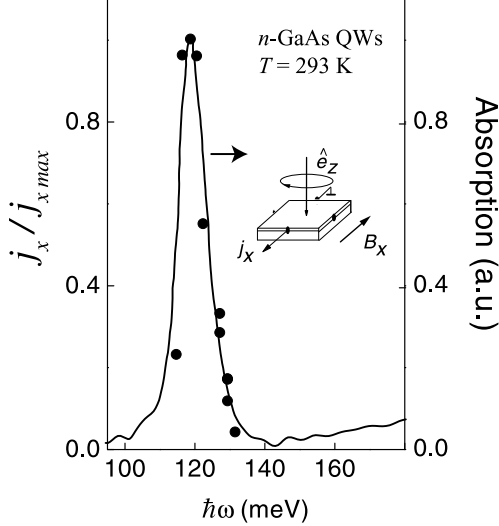


Figure 20: Spectral dependence of the spin-galvanic effect (001)-grown *n*-type GaAs QWs of 8.2 nm width at room temperature. Data (dots) are presented for optical excitation at normal incidence of right-handed circularly polarized radiation. A magnetic field of $B_x = 1$ T was used. For comparison the absorption spectrum is shown by the full line.

has been obtained in *n*-type GaAs and InAs QWs using FIR radiation (see Figs. 16-19). The presence of the spin-galvanic effect which is due to spin orientation excitable at MIR and FIR wavelengths gives clear evidence that direct inter-subband and Drude absorption of circularly polarized radiations results in spin orientation. The mechanism of this spin orientation is not obvious and will be introduced in section 4.3.2.

4.2.2 Spin-galvanic effect at optical excitation without external fields

In the experiments described above an external magnetic field was used for re-orientation of an optically generated spin polarization. The spin-galvanic effect can also be observed at optical excitation only, without application of an external magnetic field. The necessary in-plane component of the spin polarization is obtained by oblique incidence of the exciting circular polarized radiation. In this case, however, a spin orientation induced CPGE may also occur interfering with the spin-galvanic effect. Nevertheless, a pure spin-galvanic current may be obtained at inter-subband transitions in *n*-type GaAs QWs [31]. As shown above the spectrum of CPGE changes sign and vanishes in the center of resonance [24] (see section 4.1.2 and Eqs. (22) - (23)). In contrast, the optically induced spin-galvanic current is proportional to the absorbance (Eqs. (29)) and, hence, assumes a maximum at the center of the resonance [40,41] (see section 4.2.1). Thus, if a measurable helicity dependent current is present in the center of the resonance it must be attributed to the spin-galvanic effect.

These experiments have been carried out making use of the spectral tunability of the free electron laser "FELIX" [103]. The photon energy dependence of the current was measured for incidence in two different planes with components of propagation along the *x*- and *y*-directions. In Fig. 21 the observed current for both directions is plotted as a function of photon energy $\hbar\omega$ for σ_+ radiation together with the absorption spectrum. It can be seen that for a current along $x \parallel [1\bar{1}0]$ the spectral shape is similar to the derivative of the absorption spectrum, and in particular there is a change of sign which occurs at the line center of the absorption. When the sample was rotated by 90° about *z* the sign change in the current, now along $y \parallel [110]$, disappears and its spectral shape follows more closely the absorption spectrum.

The spectral inversion of sign of the photocurrent in *x* direction indicates the CPGE which is proportional to the derivative of the absorption spectrum (see Eqs. (22) and (23)). In contrast with the CPGE the sign of the spin-galvanic current does not depend on the wavelength (see section 4.2.1 and [40,41]). This can be seen from Fig. 5b which illustrates the origin of the spin-galvanic effect. All that is required is a spin orientation of the lower subband, and asymmetrical

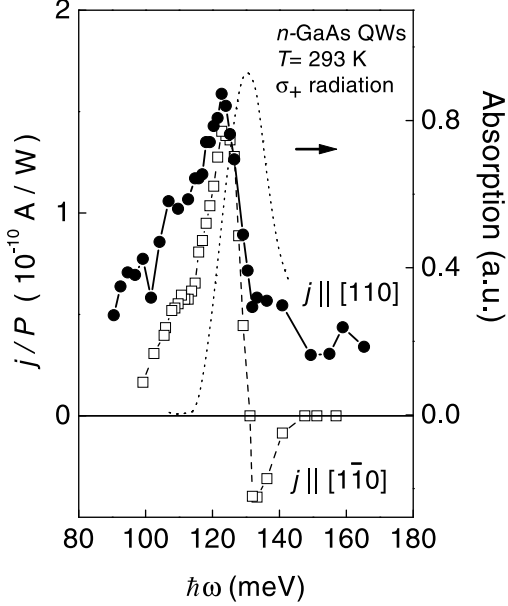


Figure 21: Photocurrent in QWs normalized by the light power P at oblique incidence of right-handed circularly polarized radiation on n -type (001)-grown GaAs/AlGaAs QWs of 8.2 nm width at $T = 293$ K as a function of the photon energy $\hbar\omega$. Circles: current in $[110]$ direction in response to irradiation parallel $[1\bar{1}0]$. Rectangles: current in $[1\bar{1}0]$ direction in response to irradiation parallel $[110]$. The dotted line shows the absorption measured using a Fourier transform spectrometer.

spin relaxation then drives a current [29]. In our case the spin orientation is generated by resonant spin-selective optical excitation followed by spin-non-specific thermalization. The magnitude of the spin polarization and hence the current depends on the initial absorption strength but not on the momentum \mathbf{k} of transition. Therefore there is no sign change and the shape of the spectrum follows the absorption (see Eqs. (29) and [31, 40, 41]). The lack of a sign change for current along $y \parallel [110]$ in the experiment shows that the spin-galvanic dominates for this orientation.

The non-equivalence of the two orientations $[110]$ and $[1\bar{1}0]$ is caused by the interplay of BIA and SIA terms in the Hamiltonian when rotating the wavevector in the QW plane. Both currents, CPGE and the spin-galvanic current, are due to spin splitting of subbands in \mathbf{k} -space described by Eq. (1). The pseudo-tensors $\boldsymbol{\gamma}$ and \mathbf{Q} determining the current are related to the transposed pseudo-tensor $\boldsymbol{\beta}$. They are subjected to the same symmetry restrictions so that their irreducible components differ only by scalar factors. In C_{2v} symmetry usually $\beta_{yx} \neq \beta_{xy}$ and it is reasonable to introduce symmetric and anti-symmetric tensor components $\beta_{BIA}^{(\nu)} = 1/2(\beta_{xy}^{(\nu)} + \beta_{yx}^{(\nu)})$ and $\beta_{SIA}^{(\nu)} = 1/2(\beta_{xy}^{(\nu)} - \beta_{yx}^{(\nu)})$, where $\nu=1,2$ indicates the $e1$ and $e2$ subbands respectively. $\beta_{BIA}^{(\nu)}$ and $\beta_{SIA}^{(\nu)}$ result from bulk inversion asymmetry (BIA) and from structural inversion asymmetry (SIA), respectively.

As discussed above and sketched in Fig. 5 both CPGE and spin-galvanic currents, say in x direction, are caused by the band splitting in k_x direction and therefore are proportional to β_{yx} (for current in y -direction one should interchange the indices x and y). Then the currents in the x and y directions read

$$j_x = A_{CPGE}[(\beta_{BIA}^{(1)} - \beta_{SIA}^{(1)}) - (\beta_{BIA}^{(2)} - \beta_{SIA}^{(2)})]P_{circ}\hat{e}_y + A_{SGE}(\beta_{BIA}^{(1)} - \beta_{SIA}^{(1)})S_y \quad (33)$$

and

$$j_y = A_{CPGE}[(\beta_{BIA}^{(1)} + \beta_{SIA}^{(1)}) - (\beta_{BIA}^{(2)} + \beta_{SIA}^{(2)})]P_{circ}\hat{e}_x + A_{SGE}(\beta_{BIA}^{(1)} + \beta_{SIA}^{(1)})S_x, \quad (34)$$

where A_{CPGE} and A_{SGE} are factors related to $\boldsymbol{\gamma}$ and \mathbf{Q} , respectively, and a subscript SGE indicates the spin-galvanic effect.

In the present case \mathbf{S} is obtained by optical orientation, its sign and magnitude are proportional to P_{circ} and it is oriented along the in-plane component of \hat{e} . The magnitude of CPGE is determined by the values of \mathbf{k} in the initial and final states, and hence depends on the spin splitting β_{BIA} and

β_{SIA} of both $e1$ and $e2$ subbands. In contrast, the spin-galvanic effect is due to relaxation between the spin states of the lowest subband and hence depends only on β_{BIA} and β_{SIA} of $e1$.

The equations above show that in directions y and x the spin-galvanic effect and the CPGE are proportional to terms with the sum and the difference respectively of BIA and SIA terms. For our sample it appears that in the case where they add, the spin-galvanic effect dominates over CPGE consistent with the lack of sign change for the current along the y -direction in Fig. 21. Conversely when BIA and SIA terms subtract the spin-galvanic effect is suppressed and CPGE dominates. We emphasize that at the maximum of absorption, where spin orientation induced CPGE is equal to zero for both directions, the current obtained is caused solely by the spin-galvanic effect.

4.3 Monopolar spin orientation

Absorption of circularly polarized light in semiconductors may result in spin polarization of photoexcited carriers. While this phenomenon of optical orientation caused by inter-band transitions in semiconductors is known since a long time [8, 109–111] and has been widely studied [3], it is not obvious that free carrier absorption due to inter-subband and intra-subband transitions can also result in a spin polarization. Observation of a spin-polarization induced CPGE and the spin-galvanic effect in the MIR and FIR spectral range unambiguously demonstrates that spin orientation may be achieved due to free carrier absorption. This optical orientation may be referred to as ‘monopolar’ [36] because photon energies are much less than the fundamental energy gap and only one type of carriers, electrons or holes, is excited. Here we consider mechanisms of monopolar optical orientation due to direct inter-subband transitions as well as by Drude-like intra-subband absorption for n - and p -type QWs based on zinc-blende structure semiconductors.

Monopolar spin orientation in n -type QWs becomes possible if an admixture of valence band states to the conduction band wave function and the spin-orbit splitting of the valence band are taken into account [40, 41]. We emphasize that the spin generation rate under monopolar optical orientation depends strongly on the energy of spin-orbit splitting of the valence band, Δ_{so} . It is due to the fact that the Γ_8 valence band and the Γ_7 spin-orbit split-off band contribute to the matrix element of spin-flip transitions with opposite signs. In p -type QWs analogous mechanisms are responsible for spin orientation.

The generation rate of the electron spin polarization \mathbf{S} due to optical excitation can be written as

$$\dot{S} = s(\eta I/\hbar\omega)P_{circ}, \quad (35)$$

where s is the average electron spin generated per one absorbed photon of circularly polarized radiation, and η is the fraction of the energy flux absorbed in the QW.

4.3.1 Direct transitions between size-quantized subbands

As Eq. (35) shows the spin generation rate \dot{S} is proportional to the absorbance η_{12} . In order to explain the observed spin orientation at inter-subband transitions between $e1$ and $e2$ subbands in n -type QWs and, in particular, the absorption of light polarized in the plane of a QW the $\mathbf{k} \cdot \mathbf{p}$ admixture of valence band states to the conduction band wave functions has to be taken into account [40, 41]. Calculations yield that inter-subband absorption of circularly polarized light propagating along z induces only spin-flip transitions resulting in 100 % optical orientation of photoexcited carriers, i.e. $s = 1$. In this geometry the fraction of the energy flux absorbed in the QW by transitions from the first subband $e1$ to the second subband $e2$ has the form

$$\eta_{12} = \frac{128\alpha^*}{9n} \frac{\Delta_{so}^2(2E_g + \Delta_{so})^2(\varepsilon_{e2} - \varepsilon_{e1})\varepsilon_{e1}}{E_g^2(E_g + \Delta_{so})^2(3E_g + 2\Delta_{so})^2} \frac{\hbar^2 n_s}{m_{e1}^*} \delta(\hbar\omega - \varepsilon_{e1} + \varepsilon_{e2}), \quad (36)$$

where α^* is the fine structure constant, n is a refraction index, n_s is a free carrier density, and ε_{e1} and ε_{e2} are the energies of the size-quantized subbands $e1$ and $e2$, respectively. The δ -function describes the resonant behaviour of the inter-subband transitions.

In p -type QWs, optical orientation is caused by heavy-hole to light-hole absorption of circularly polarized radiation and occurs for transitions at in-plane wavevector $\mathbf{k} \neq 0$ due to the mixing of heavy-hole and light-hole subbands [112].

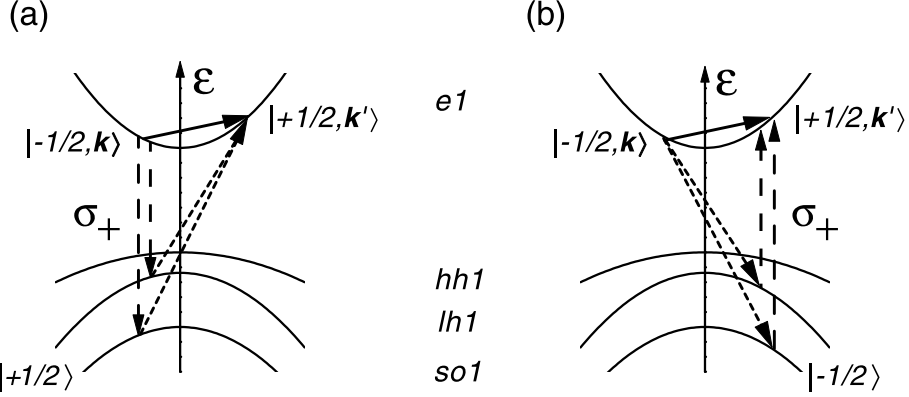


Figure 22: Sketch of indirect intra-subband optical transitions (solid arrows) with intermediate states in the valence band. Dashed and dotted arrows indicate the electron-photon interaction and the electron momentum scattering.

4.3.2 Drude absorption due to indirect intra-subband transitions

In the far-infrared range where the photon energy is not enough for direct inter-subband transition in *n*- or in *p*-type samples, the absorption of light by free carriers is caused by indirect intra-subband transitions where the momentum conservation law is satisfied due to emission or absorption of acoustic or optical phonons, static defects etc. (Drude-like absorption). We assume that the carriers occupy the *e1*-subband. The intra-subband optical transitions in QWs involving both the electron-photon interaction and momentum scattering are described by second-order processes with virtual transitions via intermediate states. The compound matrix elements for such kind of transitions with the initial and final states in the same band has the standard form [40]

$$M_{cm'_s k' \leftarrow cm_s k} = \sum_{\nu} \left(\frac{V_{cm'_s k', \nu k} R_{\nu k, cm_s k}}{\varepsilon_{\nu k} - \varepsilon_{ck} - \hbar\omega} + \frac{R_{cm'_s k', \nu k'} V_{\nu k', cm_s k}}{\varepsilon_{\nu k'} - \varepsilon_{ck} \pm \hbar\Omega_{k-k'}} \right). \quad (37)$$

Here ε_{ck} , $\varepsilon_{ck'}$ and ε_{ν} are the electron energies in the initial $|c, m_s, k\rangle$, final $|c, m'_s, k'\rangle$ and intermediate $|\nu\rangle$ states, respectively, m_s is the spin index, R is the matrix element of electron interaction with the electromagnetic wave, V is the matrix element of electron-phonon or electron-defect interaction, and $\hbar\Omega_{k-k'}$ is the energy of the involved phonon. The sign \pm in Eq. (37) correspond to emission and absorption of phonons. A dominant contribution to the optical absorption is caused by processes with intermediate states in the same subband. This is the channel that determines the coefficient of intra-subband absorbance, η . However such transitions conserve the electronic spin and, hence, do not lead to an optical orientation.

In order to obtain optical orientation due to intra-subband transitions at normal incidence we consider virtual inter-band transitions with intermediate states in the valence band [40, 41]. Fig. 22 demonstrates schematically the spin orientation at intra-band absorption of right handed circularly polarized light (σ^+) at normal incidence. Because of the dipole selection rules for inter-band optical transitions, the electron transitions with spin reversal from $m_s = -1/2$ to $m_s = +1/2$ are possible via intermediate states in the light-hole and spin-orbit split subbands, while the opposite processes, $+1/2 \rightarrow -1/2$ are forbidden. As a result spin orientation of electrons occurs. At oblique incidence, the transitions via heavy-hole subbands also contribute to optical orientation.

For this particular mechanism of monopolar optical orientation one can derive the following expression for the spin generated per one absorbed photon of e.g. right-handed circularly polarized radiation

$$s \propto \frac{V_{cv}^2}{V_c^2} \frac{\hbar\omega \Delta_{so}^2}{E_g(E_g + \Delta_{so})(3E_g + 2\Delta_{so})}. \quad (38)$$

Here V_c and V_{cv} are the intra-subband and inter-band matrix elements, respectively, and depend on the mechanism of momentum scattering. Acoustical-phonon-assisted and static impurities processes are considered in [40, 41].

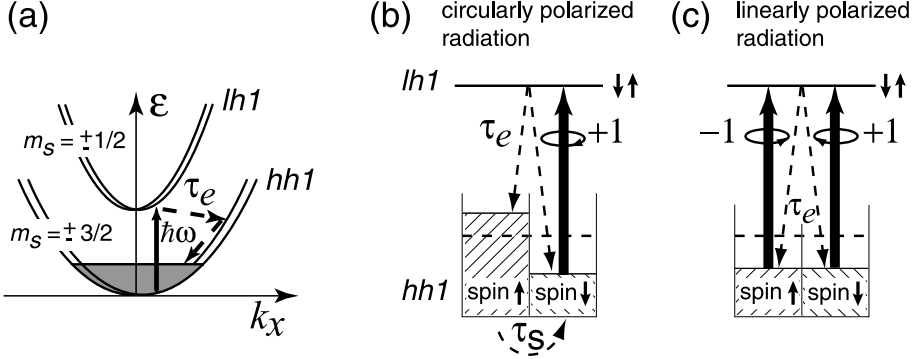


Figure 23: Microscopic picture of spin-sensitive bleaching: (a) sketch of direct optical transitions (full line) between $hh1$ and $lh1$ in p -type GaAs/AlGaAs QWs. (b) and (c) sketches the process of bleaching for circular and linear polarized radiation, respectively. Dashed arrows indicate energy (τ_e) and spin (τ_s) relaxation.

4.4 Spin controlled nonlinearity of spin orientation induced CPGE

Here we discuss the nonlinear behaviour of the spin polarization induced CPGE. It was observed in [37, 38] that the photocurrent saturates with increasing of the light intensity. In fact, in this case, the photogalvanic current normalized by the radiation intensity I is proportional to the absorbance [21] and reflects the power dependence of the absorption coefficient.

The saturation effect was investigated on p -doped QW structures at direct inter-subband optical transitions. The basic physics of spin sensitive bleaching of absorption is sketched in Fig. 23. Excitation with FIR radiation results in direct transitions between heavy-hole $hh1$ and light-hole $lh1$ subbands. This process depopulates and populates selectively spin states in $hh1$ and $lh1$ subbands. The absorption is proportional to the difference of populations of the initial and final states. At high intensities the absorption decreases since the photoexcitation rate becomes comparable to the non-radiative relaxation rate to the initial state. Due to selection rules only one type of spins is involved in the absorption of circularly polarized light. Thus the absorption bleaching of circularly polarized radiation is governed by energy relaxation of photoexcited carriers and spin relaxation in the initial state (see Fig. 23b). These processes are characterized by energy and spin relaxation times τ_e and τ_s , respectively. We note, that during energy relaxation to the initial state in $hh1$ the holes lose their photoinduced orientation due to rapid relaxation [113]. Thus, spin orientation occurs in the initial subband $hh1$, only. In contrast to circularly polarized light, absorption of linearly polarized light is not spin selective and the saturation is controlled by the energy relaxation only (see Fig. 23c). If τ_s is larger than τ_e bleaching of absorption becomes spin sensitive and the saturation intensity of circularly polarized radiation drops below the value of linear polarization.

The difference in absorption bleaching for circularly and linearly polarized radiation has been observed experimentally employing the spin orientation induced CPGE (see section 2.2) and the linear photogalvanic effect (see section 5.1) [38]. Fig. 24 shows that the photocurrent j_x measured on p -type GaAs QWs depends on the intensity I as $j_x \propto I/(1 + I/I_s)$, where I_s is the saturation intensity. It has been shown that saturation intensities I_s for circularly polarized radiation are generally smaller than that for linearly polarized radiation (Fig. 25). The non-linear behaviour of photogalvanic current has been analyzed in terms of excitation-relaxation kinetics taking into account both optical excitation and non-radiative relaxation processes. It has been shown that the photocurrent j_{LPGE} induced by linearly polarized radiation is described by $j_{LPGE}/I \propto (1 + I/I_{se})^{-1}$, where I_{se} is the saturation intensity controlled by energy relaxation of the hole gas. The photocurrent j_{CPGE} induced by circularly polarized radiation is proportional to $(1 + I \left(\frac{1}{I_{se}} + \frac{1}{I_{ss}} \right))^{-1}$ where $I_{ss} = \hbar \omega p_s / (\alpha_0 d \tau_s)$ is the saturation intensity controlled by hole spin relaxation and α_0 is the absorption coefficient at low intensities. Using experimentally obtained I_{ss} together with the absorption coefficient α_0 , calculated after [114], spin relaxation times τ_s have been derived (see Fig. 26) [38]. We note that in the definition of I_{ss} it was assumed that the spin selection rule are fully satisfied at the transition energy. This is the case for optical transitions occurring close to $\mathbf{k} = 0$ [113] being realized in the above experiment. If this is not the case the mixture of heavy-

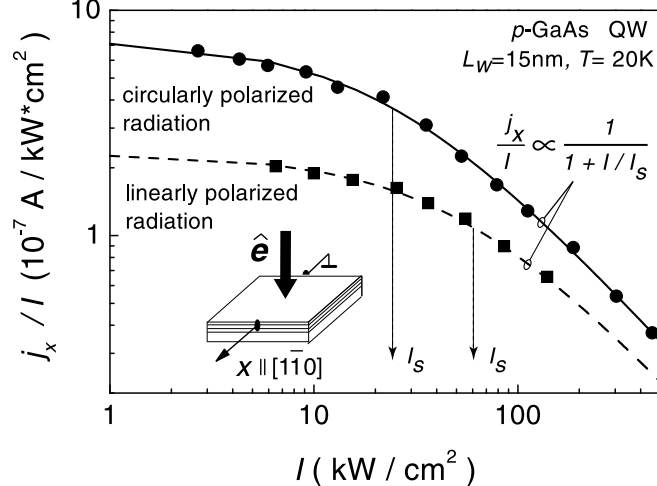


Figure 24: CPGE and LPGE currents j_x normalized by intensity I as a function of I for circularly and linearly polarized radiation of $\lambda = 148 \mu\text{m}$, respectively. The inset shows the geometry of the experiment. The current j_x is measured along $[1\bar{1}0]$ at normal incidence of radiation on p -type (113)A-grown GaAs QW with $L_W = 15 \text{ nm}$ at $T = 20 \text{ K}$. LPGE was obtained with the electric field vector \mathbf{E} oriented at 45° to the x -direction (see Eqs. (44)) was used. The measurements are fitted to $j_x/I \propto 1/(I + I/I_s)$ with one parameter I_s for each state of polarization (full line: circular, broken line: linear).

hole and light-hole subbands reduces the strength of the selection rules [73] and therefore reduces the efficiency of spin orientation. The mixing yields a multiplicative factor in I_{ss} increasing the saturation intensity at constant spin relaxation time [37]. In [115] a substantial lowering of I_{ss} with decreasing QW width was observed. This observation may indicate much slower spin relaxation times for holes in narrow QWs as obtained theoretically in [113].

This result shows that spin relaxation of holes may be obtained by investigation of the circular photogalvanic effect as a function of radiation intensity. A substantial portion of investigations of the spin lifetime in semiconductor devices are based on optical spin orientation by inter-band excitation and further tracing the kinetics of polarized photoluminescence (for review see [1, 3, 116, 117]). These studies give important insights into the mechanisms of spin relaxation of photoexcited free carriers. In contrast to these methods of optical spin orientation, monopolar spin orientation allows to study spin relaxation without electron-hole interaction and exciton formation in the conditions close to the case of electric spin injection [29, 38, 39]. Spin photocurrents provide an experimental access to such investigations.

5 Spin-independent photocurrents at homogeneous excitation

Investigating spin photocurrents one should take into account that optical excitation may generate other currents which are not the result of spin orientation. Spin photocurrents can be recognized by their dependence on the helicity of the exciting radiation. Indeed, only spin photocurrents change their direction when the state of polarization of radiation is switched from right- to left-handed or vice versa. This allows to extract the spin photocurrent contribution from total photocurrents at visible excitation when spin-independent photocurrents, like in the case of Dember-effect or photo-voltaic effect at contacts etc., may occur, being substantially larger than spin photocurrents. In this situation the periodic modulation of the state of polarization and synchronous detection of the current is a convenient technique to measure spin photocurrents by itself. In the infrared spectral range these strong spin-independent photocurrents do not occur. However, there are two other sources of photocurrents at homogeneous excitation which occur simultaneously and may be of the same order of magnitude as spin photocurrents but again do not require spin orientation. These are the linear photogalvanic effect (LPGE) [13, 14] and the photon drag effect [118, 119]. These photocurrents are not changed in sign or amplitude if the polarization is switched from

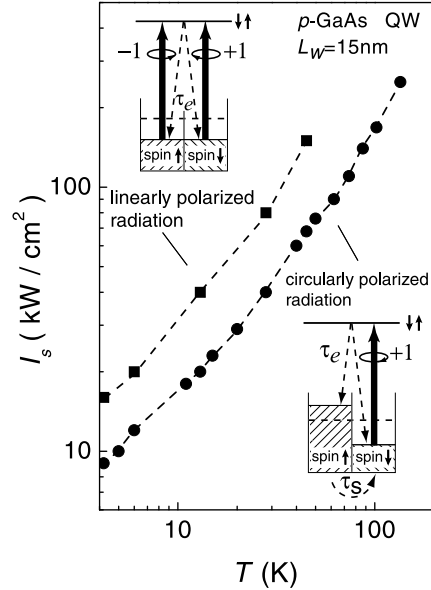


Figure 25: Temperature dependence of the saturation intensity I_s for linearly and circularly polarized radiation of $\lambda = 148\mu\text{m}$. The dependence is shown for a *p*-type GaAs/AlGaAs (113)A-grown sample with a single QW of $L_W=15$ nm width. The free carrier density and the mobility were $1.66 \cdot 10^{11} \text{ cm}^{-2}$ and $6.5 \cdot 10^5 \text{ cm}^2/(\text{Vs})$, respectively.

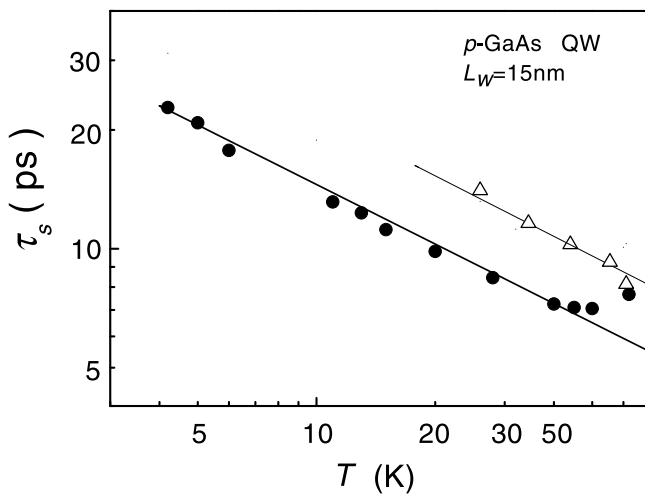


Figure 26: Experimentally determined spin relaxation times τ_s of holes in *p*-type GaAs/AlGaAs QWs as a function of temperature T . Open triangles and full dots correspond to (113)A-grown 15 nm single and multiple (20) QWs, respectively. Free carrier densities of all samples were about $2 \cdot 10^{11} \text{ cm}^{-2}$ for each QW.

σ_+ to σ_- . Furthermore both effects, LPGE and photon drag effect, depend on the symmetry of the material in a different way than spin photocurrents. Therefore in most cases it is possible to choose a crystallographic orientation and an experimental geometry where only spin photocurrents occur. In other cases the helicity dependence of photocurrents allows to distinguish between spin photocurrents and spin-independent photocurrents. Based on phenomenology we discuss spin-independent photocurrents in the following and present some experimental examples.

By general symmetry arguments it can be shown that these spin-independent photocurrents are given by

$$j_\lambda = \sum_{\mu\nu} \chi_{\lambda\mu\nu} (E_\mu E_\nu^* + E_\nu E_\mu^*)/2 + \sum_{\delta\mu\nu} T_{\lambda\delta\mu\nu} q_\delta E_\mu E_\nu^*. \quad (39)$$

where $\chi_{\lambda\mu\nu}$ and $T_{\lambda\delta\mu\nu}$ are components of a third rank and a fourth rank tensor, respectively, and q_δ is the wavevector of the radiation in the sample.

The first term on the right-hand side of Eq. (39) is called LPGE because it is independent on the sign of circular polarization and is usually measured by linearly polarized radiation. The second term represents the photon drag effect which yields a current due to momentum transfer from photons to electrons.

5.1 Linear photogalvanic effect

LPGE arises in homogeneous samples under homogeneous excitation due to an asymmetry of the scattering of free carriers on phonons, static defects, or other carriers in non-centrosymmetric media (for review see [13, 14]). The linear photogalvanic effect was observed in some insulators as early as the 1950th, but was correctly identified as a new phenomenon only in [120] and theoretically treated in [121]. In bulk materials like GaAs LPGE was studied in great detailed (for review see [11–14]). It has also been considered and observed in low dimensional structures like MOSFET Si-structures [122, 123], III-V QWs [10, 21, 35, 124] and asymmetric SiGe QWs [23]. Microscopically, the LPGE current consists of a so-called ballistic and a shift contribution [125–127]. The LPGE was successfully applied as a fast detector of the degree of circular polarization [128, 129].

As shown in Eq. (39) the linear photogalvanic current is linked to the symmetrized product $E_\mu E_\nu^*$ by a third rank tensor $\chi_{\lambda\mu\nu}$ which in turn is symmetric in the last two indices. Therefore $\chi_{\lambda\mu\nu}$ is isomorphic to the piezoelectric tensor and may have non-zero components in media lacking a center of symmetry. Note that in contrast to spin photocurrents gyrotropy is not necessary. In zinc-blende structure based QWs of C_{2v} symmetry taking into account only the LPGE term of Eq. (39) we get

$$j_{LPGE,x} = \chi_{xxz} (E_x E_z^* + E_z E_x^*) , \quad j_{LPGE,y} = \chi_{yyz} (E_y E_z^* + E_z E_y^*) . \quad (40)$$

In higher symmetry QWs of point-group D_{2d} the coefficients are linearly dependent and $\chi_{xxz} = -\chi_{yyz}$. Eqs. (40) shows that the LPGE occurs only at oblique incidence of radiation because a component of the electric field, E_z , along the z -axis is required.

We assume now irradiation of a QW of the C_{2v} symmetry with the plane of incidence parallel to (yz) . For linearly polarized light with an angle α between the plane of polarization defined by the electric field vector and the x -coordinate parallel to $[1\bar{1}0]$ the LPGE current is given by:

$$j_{LPGE,x} = \chi_{xxz} \hat{e}_y E_0^2 \sin 2\alpha , \quad j_{LPGE,y} = (\chi_+ + \chi_- \cos 2\alpha) \hat{e}_y E_0^2 , \quad (41)$$

where $\chi_\pm = (\chi_{xxz} \pm \chi_{yyz})/2$. In the experimental setup used for the measurement of the helicity dependence of spin photocurrents the laser light is linearly polarized along x and a $\lambda/4$ plate is placed between the laser and the sample, Eqs. (40) take the form

$$j_{LPGE,x} = \chi_{xxz} \hat{e}_y E_0^2 \cos 2\varphi \sin 2\varphi , \quad j_{LPGE,y} = (\chi_+ + \chi_- \cos 2\varphi) \hat{e}_y E_0^2 , \quad (42)$$

In addition to Eqs. (40) the point group C_s allows an LPGE current at normal incidence of the radiation because in this case the tensor χ has the additional non-zero components $\chi_{xxy'} = \chi_{xy'x}$, $\chi_{y'xx}$ and $\chi_{y'y'y'}$. This current is given by

$$j_{LPGE,x} = \chi_{xxy'} (E_x E_{y'}^* + E_{y'} E_x^*) , \quad j_{LPGE,y'} = (\chi_{y'xx} |E_x|^2 + \chi_{y'y'y'} |E_{y'}|^2) \quad (43)$$

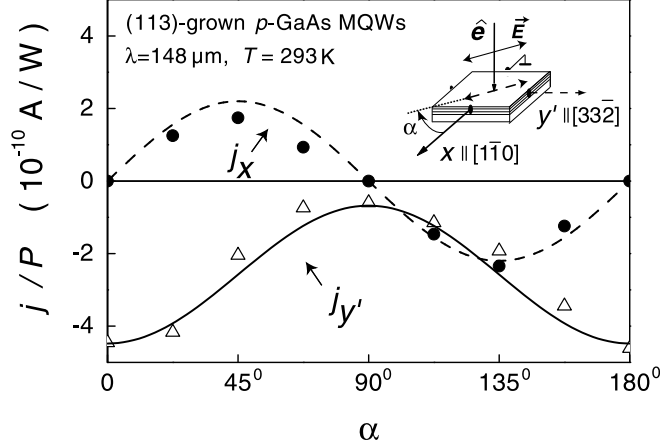


Figure 27: Linear photogalvanic current j normalized by P as a function of the angle α between the plane of linear polarization and the axis x . Data are obtained for x and y' direction under normal incidence. The broken line and the full line are fitted after Eqs. (44).

yielding for linearly polarized light

$$j_{LPGE,x} = \chi_{xxy'} \hat{e}_{z'} E_0^2 \sin 2\alpha, \quad j_{LPGE,y'} = (\chi'_+ + \chi'_- \cos 2\alpha) \hat{e}_{z'} E_0^2, \quad (44)$$

where $\chi'_\pm = (\chi_{xxx} \pm \chi_{xy'y'})/2$ and for the experimental arrangement of helicity dependence measurements

$$j_{LPGE,x} = \chi_{xxy'} \hat{e}_{z'} E_0^2 \cos 2\varphi \sin 2\varphi, \quad j_{LPGE,y'} = (\chi'_+ + \chi'_- \cos 2\varphi) \hat{e}_{z'} E_0^2, \quad (45)$$

The dependence of the LPGE current on the angle of incidence Θ_0 is determined by the projections of the unit vector \hat{e} which, as in the case of CPGE, have the form of Eqs. (16)-(18).

Eqs. (42) and (45) for LPGE at excitation with elliptically polarized radiation show that it may occur simultaneously with spin orientation induced CPGE (see Eqs. (14) and (15)). However, in this case LPGE is equal to zero for circularly polarized radiation for all considered symmetries. Indeed, light is circularly polarized at $2\varphi = \pi/2, 3\pi/2 \dots$ therefore for σ_\pm radiation $\cos 2\varphi$ in Eqs. (42) and (45) is equal to zero and the LPGE current vanishes. For P_{circ} between -1 and +1, as in the measurements of helicity dependence of the photocurrent both, spin orientation induced CPGE and LPGE can be simultaneously present. However, measurements carried out on GaAs [10, 20-22], InAs [20, 21], and ZnSeMnTe [43] QWs in the whole wavelength range as well as on SiGe QWs in the mid infrared [23, 107] have shown that the contribution of the LPGE is negligible (see Figs. 10 and 13).

The situation is different for SiGe QWs at the FIR excitation where spin orientation induced CPGE and LPGE with comparable strength have been detected [23, 107]. Fig. 15 exhibits experimental data obtained on p -type SiGe (113)-grown QW structure. Broken and dotted lines show contributions of the circular photocurrent, $j_x \propto \sin 2\varphi$, and the linear photocurrent, $j_x \propto \sin 2\varphi \cdot \cos 2\varphi$, respectively. The tensors γ and χ describe different physical mechanisms and, therefore, may depend differently on the material parameters, excitation wavelength, and temperature. Obviously in most cases the contribution of γ to the photocurrent is larger than that of χ .

The occurrence of LPGE without CPGE is demonstrated by measurements at linear polarization at which CPGE is zero, depicted in Fig. 27 for GaAs QWs and in Fig. 28 for SiGe QWs. It was also observed at the excitation by elliptical polarized radiation with P_{circ} varying from -1 to +1 in a geometrical direction where CPGE is forbidden by symmetry. This is demonstrated in Fig. 29 where a longitudinal current generated by oblique incidence along [110] direction is shown.

5.2 Photon drag effect

The photon drag effect arises due to a momentum transfer from photons to free carriers. This effect was first observed in bulk semiconductors [130, 131] and has been investigated in various materials

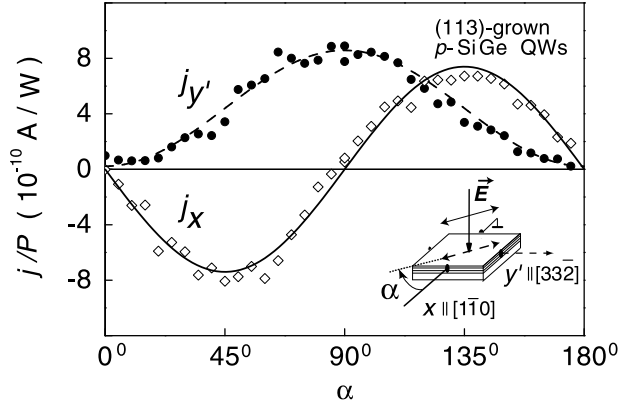


Figure 28: Linear photogalvanic current j normalized by P for x and y' direction as a function of the angle α between the plane of linear polarization and the axis x . The results were obtained at room temperature with (113)-grown SiGe QWs under normal incidence of irradiation at $\lambda = 280 \mu\text{m}$. The broken line and the full line are fitted after Eqs. (44).

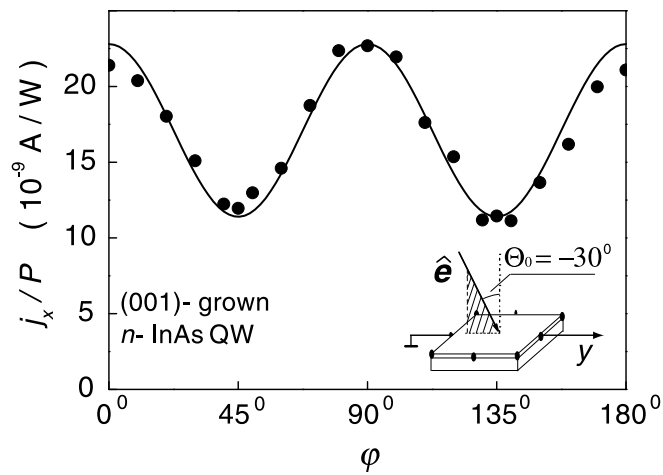


Figure 29: Linear photogalvanic current j_y normalized by P as a function of the phase angle φ . The solid curve is fitted after Eq. (42).

like Ge, Si and GaP in a wide range of optical excitation mechanisms as inter-band transitions, direct and indirect transitions at free carrier absorption, at impurity ionization etc. (for review see [118, 119]). It was also intensively studied in GaAs and InAs QWs [21, 132–139]. The photon drag is of great technical importance for fast infrared and far-infrared detection of short laser pulses [104, 105, 118, 119, 140].

The photon drag current described by the second term of the right hand side of Eq. (39) is mediated by a fourth rank tensor \mathbf{T} . Therefore there is no symmetry restriction for this effect. In $T_{\lambda\delta\mu\nu}$ the first index λ runs over x and y only because the current must be confined in the plane of the QW.

For QWs of C_{2v} symmetry the photon drag effect yields the current

$$\begin{aligned} j_{PD,x} &= \sum_{\mu=x,y,z} T_{xx\mu\mu} q_x |E_\mu|^2 + T_{xyxy} q_y (E_x E_y^* + E_y E_x^*) , \\ j_{PD,y} &= \sum_{\mu=x,y,z} T_{yy\mu\mu} q_y |E_\mu|^2 + T_{yxyx} q_x (E_x E_y^* + E_y E_x^*) . \end{aligned} \quad (46)$$

For C_s symmetry this equation has the same form if y and z are replaced by the primed coordinates. In higher symmetric QWs of the point group D_{2d} the number of independent non-zero tensor components is reduced by

$$T_{xxxx} = T_{yyyy} , \quad T_{xxyy} = T_{yyxx} , \quad T_{xxzz} = T_{yyzz} , \quad T_{xyxy} = T_{yxyx} . \quad (47)$$

The above equations show that the photon drag effect occurs in QWs of all symmetries at oblique incidence of radiation only. The longitudinal effect, first term on the right hand side of Eqs. (46), is usually much stronger than the transverse effect described by the second term. This is the reason that in the transverse geometry of spin orientation induced CPGE no influence of the photon drag effect could be detected as yet. However, in the longitudinal geometry the photon drag effect yields a measurable current. Again helicity dependence can help to distinguish spin photocurrents from the photon drag effect. On the other hand the separation of LPGE and photon drag effect is not so obvious. The usual method to identify photon drag effect is based on the sign inversion of the current by reversing the wavevector of light in the plane of the sample. The same sign inversion occurs also for LPGE (see Eqs. (16), (18), (41), and (42)).

Both effects may be distinguished from polarization dependencies. The situation is simple for transversal currents. Indeed, LPGE vanishes for linearly polarized radiation with the radiation electric field normal or parallel to the current flow (see left equation of Eqs. (41),(44)) or for circularly polarized radiation (see left equation of Eqs. (42),(45)) whereas a photon drag effect may be present (see Eqs. (46)). However, for longitudinal currents the photon drag effect and the LPGE may be present at the same time with comparable strength for any polarization. In contrast to the transverse effect, longitudinal LPGE has a polarization independent term χ_+ in the right equation of Eqs. (41),(42) and χ'_+ in the right equation of Eqs. (44),(45). Thus, a longitudinal current in non-centrosymmetric QWs which changes sign at reversal of light propagation need not to be the photon drag current. The characteristic polarization dependencies as well as the helicity dependence may help to identify the underlying microscopic mechanisms. We note that by investigation of the photon drag effect in QWs without inversion center one should *always* take into account the LPGE contribution and vice versa. For elliptical polarization the spin orientation induced CPGE may also contribute in the total current.

As a concluding remark, spin photocurrents in any case can be distinguished from helicity independent currents by switching the helicity from right to left or the other way round. The fraction of spin photocurrents in the total current can quantitatively be extracted by modulation methods.

6 Spin photocurrents caused by inhomogeneities

One of the essential features of spin photocurrents reviewed here is the homogeneity of both the optical excitation and the distribution of spin polarization in a two-dimensional electron gas of gyrotropic QWs. However, spin photocurrents may occur due to an inhomogeneous spin distribution obtained by inhomogeneous optical excitation or in bulk inhomogeneities like $p - n$ junctions.

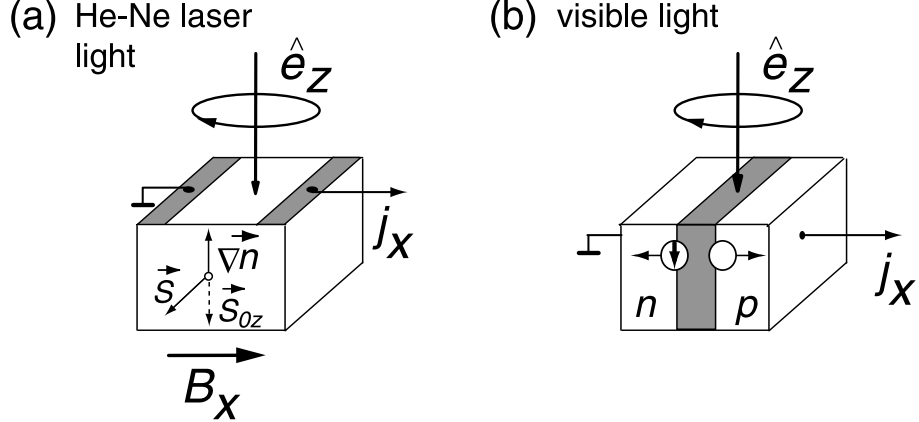


Figure 30: Sketches of the experimental arrangement of: (a) Surface spin photocurrent due to non-homogeneous spin orientation after [9]. ∇n indicates gradient of electron density in the penetration depth of strong fundamental absorption. (b) Spin-voltaic effect after [141, 142]. Circle with arrow indicates spin polarized electrons, open circle represents unpolarized holes due to rapid spin relaxation.

As it was already introduced a surface current $\mathbf{j} = e \cdot \zeta \cdot \text{rot} \mathbf{S}$ due to inhomogeneity of spin polarization \mathbf{S} of electrons at a semiconductor surface layer proposed in [7] was observed in bulk AlGaAs samples [9]. Here ζ is a coefficient proportional to the energy of the spin-orbit splitting of the valence band Δ_{so} . The inhomogeneous spin polarization was obtained by the strong absorption of circularly polarized radiation at the band edge of AlGaAs mixed crystals (HeNe-laser excitation). The radiation was of normal incidence on the sample resulting in a gradient of the spin density into the material due to surface generation and diffusion into the bulk. Spin-orbit interaction at the surface yields asymmetric electron scattering which gives rise to a current in the direction perpendicular to the gradient of spin density and the average electron spin. An external magnetic field oriented in the surface plane was used to optimize the current by rotating the spin polarization into the surface plane (see Fig. 30a) [9]. The surface current shows the Hanle-effect as a function of the magnetic field strength. The geometry and the experimental procedure are very similar to that used to demonstrate the spin-galvanic effect (see Fig. 7). The crucial difference to the spin-galvanic effect is that in this case of surface photocurrent caused by optical orientation a gradient of spin density is needed. Naturally this gradient is absent in QWs where the spin-galvanic effect has been investigated because QWs are two-dimensional (no ‘thickness’).

Another type of spin photocurrents recently was proposed in analogy to the photo-voltaic effect in $p - n$ junctions [141, 142]. This spin-voltaic effect occurs due to uniform illumination of a $p - n$ junction with circularly polarized inter-band light resulting in spin polarization of a charge current. Circular polarization generates spin polarized electrons and holes. Due to the fast relaxation of hole spin polarization in the bulk and the long spin lifetime of electrons, the photocurrent becomes spin polarized. Indeed by the built-in electric field E_{bi} spin polarized electrons are swept to the n -side and the unpolarized holes drift to the p -side of the junction (see Fig. 30b).

7 Summary

A non-equilibrium uniform spin polarization obtained by optical orientation drives an electric current in QWs if they belong to a gyrotropic crystal class. In QWs prepared from zinc-blende structure materials gyrotropy is naturally given due to the lack of inversion symmetry in the basic material which itself is not gyrotropic. In QWs based on diamond structure materials, like Si and Ge which possess a center of inversion, gyrotropy may be introduced by artificially growing of asymmetric structures. In gyrotropic QWs spin-orbit interaction results in a spin splitting in \mathbf{k} -space of subbands yielding the basis of spin photocurrents. Two different microscopic mechanisms of spin photocurrents can be distinguished, spin orientation induced circular photogalvanic effect and spin-galvanic effect. In the first effect the coupling of the helicity of light to spin polarized final

states with a net linear momentum is caused by angular momentum selection rules together with band splitting in \mathbf{k} -space due to \mathbf{k} -linear terms in the Hamiltonian. The current flow in the second effect is driven by asymmetric spin relaxation of a homogeneous non-equilibrium spin polarization. The current is present even if the initial electron distribution in each spin-split subband is uniform.

The experimental results on spin photocurrents due to homogeneous spin polarization are in good agreement to the phenomenological theory. Both mechanisms of spin photocurrents as well as the removal of spin degeneracy in \mathbf{k} -space are described by second rank pseudo-tensors. Because of tensor equivalence in each symmetry the irreducible components of these tensors differ by scalar factors only. Therefore macroscopic measurements of photocurrents in different geometric configurations of experiments allow to conclude on details of the microscopic tensorial spin orbit interaction. In particular the relation between the symmetric and anti-symmetric part of the spin-orbit interaction representing Dresselhaus like terms (including interface inversion asymmetry) and the Rashba term, respectively, may be obtained. Furthermore the macroscopic symmetry of QWs may easily be determined.

Spin photocurrents are obtained by circularly polarized radiation. The most important feature of spin photocurrents is their helicity dependence. The current is proportional to helicity and reverses its direction upon changing the handedness of radiation. The effect is a quite general property of QWs and has already been observed in many different n - and p -type semiconductor structures at various kinds of optical excitation like inter-band and free carrier absorption. It is present in materials of different mobilities, also at very low mobility, in a wide range of carrier densities and can be detected even at room temperature. Spin photocurrents are not limited to 2D structures. Most recently they have been predicted for gyrotropic 1D systems like carbon nanotubes of spiral symmetry [143]. The effect is caused by coupling between the electron wavevector along the tube principal axis and the orbital momentum around the tube circumference.

Spin photocurrents were applied to investigate the mechanism of spin relaxation at monopolar spin orientation where only one type of charge carriers is involved in the excitation-relaxation process. This condition is close to that of electrical spin injection in semiconductors. Two methods were applied to determine spin relaxation times: the Hanle effect in the spin-galvanic current and spin sensitive bleaching of photogalvanic currents. The spin orientation induced CPGE has also been applied to detect the state of polarization of terahertz radiation [42]. The rapid momentum relaxation at room temperature in quantum well yields picosecond time resolution.

Acknowledgement

The authors thank E.L. Ivchenko, V.V. Bel'kov, L.E. Golub, S.N. Danilov and Petra Schneider for many discussions and helpful comments on the present manuscript. We are also indebted to G. Abstreiter, V.V. Bel'kov, M. Bichler, J. DeBoeck, G. Borghs, K. Brunner, S.N. Danilov, J. Eroms, E.L. Ivchenko, S. Giglberger, P. Grabs, L.E. Golub, T. Humbs, J. Kainz, H. Ketterl, B.N. Murdin, Petra Schneider, D. Schuh, M. Sollinger, S.A. Tarasenko, L. Molenkamp, R. Newmann, V.I. Perel, C.R. Pidgeon, P.J. Phillips, U. Rössler, W. Schoepe, D. Schowalter, G. Schmidt, V.M. Ustinov, L.E. Vorobjev, D. Weiss, W. Wegscheider, D.R. Yakovlev, I.N. Yassievich, and A.E. Zhukov, for long standing cooperation during the work on spin photocurrents. We gratefully acknowledge financial support by the Deutsche Forschungsgemeinschaft (DFG), the Russian Foundation for Basic Research (RFBR) and the NATO Linkage Grant which made this work possible.

References

- [1] *Semiconductor Spintronics and Quantum Computation*, eds. D.D. Awschalom, D. Loss, and N. Samarth, in the series *Nanoscience and technology*, eds. K. von Klitzing, H. Sakaki, and R. Wiesendanger (Springer, Berlin, 2002).
- [2] Y.A. Bychkov, and E.I. Rashba, Pis'ma ZhETF **39**, 66 (1984) [Sov. JETP Lett. **39**, 78 (1984)].
- [3] *Optical orientation*, F. Meier, and B.P. Zakharchenya, Eds. (Elsevier Science Publ., Amsterdam, 1984).

- [4] D. Hägele, M. Oestreich, W.W. Rühle, N. Nestle, and K. Eberl, *Appl. Phys. Lett.* **73**, 1580 (1998).
- [5] J.M. Kikkawa, and D.D. Awschalom, *Nature* **397**, 139 (1999).
- [6] A. Hirohata, Y.B. Xu, C.M. Guertler, and A.C. Bland, *J. Appl. Phys.* **85**, 5804 (1999).
- [7] N.S. Averkiev, and M.I. D'yakonov, *Fiz. Tekh. Poluprov.* **17**, 629 (1983) [Sov. Phys. Semicond. **17**, 393 (1983)].
- [8] M.I. D'yakonov, V.I. Perel', *Pis'ma ZhETF* **13**, 206 (1971) [Sov. JETP Lett. **13**, 144 (1971)].
- [9] A.A. Bakun, B.P. Zakharchenya, A.A. Rogachev, M.N. Tkachuk, and V.G. Fleisher, *Pis'ma ZhETF* **40**, 464 (1984) [Sov. JETP Lett. **40**, 1293 (1984)].
- [10] S.D. Ganichev, E.L. Ivchenko, H. Ketterl, W. Prettl, and L.E. Vorobjev, *Appl. Phys. Lett.* **77**, 3146 (2000).
- [11] E.L. Ivchenko, and G.E. Pikus, in *Problems of Modern Physics* (in Russian), ed. V.M. Tuchkevich and V.Ya. Frenkel, Leningrad, Nauka, 1980, p.275 [English translation: *Semiconductor Physics*, ed. V.M. Tuchkevich and V.Ya. Frenkel, Cons. Bureau, New York, 1986, p. 427].
- [12] V.I. Belinicher, and B.I. Sturman, *Usp. Fiz. Nauk* **130**, 415 (1980) [Sov. Phys. Usp. **23**, 199 (1980)].
- [13] B.I. Sturman, and V.M. Fridkin, *The Photovoltaic and Photorefractive Effects in Non-Centrosymmetric Materials*, Gordon and Breach Science Publishers, New York, 1992.
- [14] E.L. Ivchenko, and G.E. Pikus, *Superlattices and Other Heterostructures. Symmetry and Optical Phenomena*, (Springer, Berlin 1997).
- [15] E.L. Ivchenko, and G.E. Pikus, *Pis'ma ZhETF* **27**, 640 (1978) [Sov. JETP Lett. **27**, 604 (1978)].
- [16] V.I. Belinicher, *Phys. Lett. A* **66**, 213 (1978).
- [17] V.M. Asnin, A.A. Bakun, A.M. Danishevskii, E.L. Ivchenko, G.E. Pikus, and A.A. Rogachev, *Pis'ma ZhETF* **28**, 80 (1978) [Sov. JETP Lett. **28**, 74 (1978)].
- [18] V.M. Asnin, A.A. Bakun, A.M. Danishevskii, E.L. Ivchenko, G.E. Pikus, and A.A. Rogachev, *Solid State Commun.* **30**, 565 (1979).
- [19] N.S. Averkiev, V.M. Asnin, A.A. Bakun, A.M. Danishevskii, E.L. Ivchenko, G.E. Pikus, A.A. Rogachev, *Fiz. Tekh. Poluprov.* **18**, 639; 648 (1984) [Sov. Phys. Semicond. **18**, 397; 402 (1984)].
- [20] S.D. Ganichev, E. L. Ivchenko, S.N. Danilov, J. Eroms, W. Wegscheider, D. Weiss, and W. Prettl, *Phys. Rev. Lett.* **86**, 4358 (2001).
- [21] S.D. Ganichev, E.L. Ivchenko, and W. Prettl, *Physica E* **14**, 166 (2002).
- [22] S.D. Ganichev, Proceed. of ICPS-26, to be published.
- [23] S.D. Ganichev, U. Rössler, W. Prettl, E.L. Ivchenko, V.V. Bel'kov, R. Neumann, K. Brunner, and G. Abstreiter, *Phys. Rev. B* **66**, 75328 (2002).
- [24] S.D. Ganichev, V.V. Bel'kov, Petra Schneider, E.L. Ivchenko, S.A. Tarasenko, D. Schuh, W. Wegscheider, D. Weiss, and W. Prettl, submitted to *Phys. Rev. B* (cond-mat/0303054).
- [25] L.E. Golub, *Physica E*, to be published (cond-mat/0208295).
- [26] L.E. Golub, *Phys. Rev. B*, to be published.

- [27] E.L. Ivchenko, Yu.B. Lyanda-Geller, and G.E. Pikus, Pis'ma ZhETF **50**, 156 (1989) [Sov. JETP Lett. **50**, 175 (1989)].
- [28] E.L. Ivchenko, Yu.B. Lyanda-Geller, and G.E. Pikus, ZhETF **98**, 989 (1990) [Sov. Phys. JETP **71**, 550 (1990)].
- [29] S.D. Ganichev, E.L. Ivchenko, V.V. Bel'kov, S.A. Tarasenko, M. Sollinger, D. Weiss, W. Wegscheider, and W. Prettl, *Nature* (London) **417**, 153 (2002).
- [30] S.D. Ganichev, E.L. Ivchenko, V.V. Bel'kov, S.A. Tarasenko, M. Sollinger, D. Schowalter, D. Weiss, W. Wegscheider, and W. Prettl, J. of Supercond.: Incorporating Novel Magn. **16**, 369 (2003) (cond-mat/0301390).
- [31] S.D. Ganichev, Petra Schneider, V.V. Bel'kov, E.L. Ivchenko, S.A. Tarasenko, W. Wegscheider, D. Weiss, D. Schuh, D.G. Clarke, M. Merrick, B.N. Murdin, P. Murzyn, P.J. Phillips, C.R. Pidgeon, E.V. Beregulin, and W. Prettl, submitted to Phys. Rev. B. (cond-mat/0303193).
- [32] R.D.R. Bhat, and J.E. Sipe, Phys. Rev. Lett. **85**, 5432 (2000).
- [33] M.J. Stevens, A.L. Smirl, R.D.R. Bhat, J.E. Sipe, and H.M. van Driel, J. Appl. Phys. **91**, 4382 (2002).
- [34] M.V. Entin, Fiz. Tekh. Poluprov. **23**, 1066 (1989) [Sov. Phys. Semicond. **23**, 664 (1989)].
- [35] L.I. Magarill, Physica E **9**, 652 (2001).
- [36] S.D. Ganichev, H. Ketterl, and W. Prettl, Physica B **272**, 464 (1999).
- [37] S.D. Ganichev, V.V. Bel'kov, S.N. Danilov, E.L. Ivchenko, H. Ketterl, L.E. Vorobjev, M. Bichler, W. Wegscheider, and W. Prettl, Physica E **10**, 52 (2001).
- [38] S.D. Ganichev, S.N. Danilov, V.V. Bel'kov, E.L. Ivchenko, M. Bichler, W. Wegscheider, D. Weiss, and W. Prettl, Phys. Rev. Lett. **88**, 057401-1 (2002).
- [39] S.D. Ganichev, S.N. Danilov, M. Sollinger, D. Weiss, W. Wegscheider, W. Prettl, V.V. Bel'kov, and E.L. Ivchenko, MRS Symp. Proc. **690**, eds. T.J. Klemmer, J.S. Sun, A. Fert, and J. Bass, F1.2.1 (2001).
- [40] S.A. Tarasenko, E.L. Ivchenko, V.V. Bel'kov, S.D. Ganichev, D. Schowalter, Petra Schneider, M. Sollinger, W. Prettl, V.M. Ustinov, A.E. Zhukov, and L. E. Vorobjev, Proceed. of ICPS-26, to be published (cond-mat/0301393).
- [41] S.A. Tarasenko, E.L. Ivchenko, V.V. Bel'kov, S.D. Ganichev, D. Schowalter, Petra Schneider, M. Sollinger, and W. Prettl, V.M. Ustinov, A.E. Zhukov, and L.E. Vorobjev, Journal of Supercond.: Incorporating novel Magn. **16**, 419 (2003) (cond-mat/0301388).
- [42] S.D. Ganichev, H. Ketterl, and W. Prettl, Int. J. Infared and MM Waves, to be published.
- [43] S.D. Ganichev, M. Sollinger, W. Prettl, D.R. Yakovlev, P. Grabs, G. Schmidt, L. Molenkamp, and E.L. Ivchenko, Verhandl. DPG (VI) 36, 1/170 (2001).
- [44] D. Stein, K. von Klitzing, and G. Weimann, Phys. Rev. Lett. **51**, 130 (1983).
- [45] H.L. Stormer, Z. Schlesinger, A. Chang, D.C. Tsui, A.C. Gossard, and W. Wiegmann, Phys. Rev. Lett. **51**, 126 (1983).
- [46] M.I. D'yakonov, and V.Yu. Kachorovskii, Fiz. Tekh. Poluprov. **20**, 178 (1986) [Sov. Phys. Semicond. **20**, 110 (1986)].
- [47] N.S. Averkiev, L.E. Golub, and M. Willander, J. Phys.: Condens. Matter **14**, R271 (2002).
- [48] A. Voskoboinikov, S.S. Liu, and C.P. Lee, Phys. Rev. B **58**, 15397 (1998).

- [49] E.A. de Andrada e Silva, G.C. La Rocca, Phys. Rev. B **59**, 15583 (1999).
- [50] T. Koga, J. Nitta, H. Takayanagi, and S. Datta, Phys. Rev. Lett. **88**, 126601 (2002).
- [51] V.I. Perel', S.A. Tarasenko, I.N. Yassievich, S.D. Ganichev, V.V. Bel'kov, and W. Prettl, submitted to Phys. Rev. B. (cond-mat/ 0301098).
- [52] V.K. Kalevich, and V.L. Korenev, Pis'ma ZhETF **52**, 859 (1990) [Sov. JETP Lett. **52**, 230 (1990)].
- [53] J. Nitta, T. Akazaki, and H. Takayanagi, Phys. Rev. Lett. **78**, 1335 (1997).
- [54] J.P. Lu, J.B. Yau, S.P. Shukla, M. Shayegan, L. Wissinger, U. Rössler, and R. Winkler, Phys. Rev. Lett. **81**, 1282 (1998).
- [55] J.P. Heida, B.J. van Wees, J.J. Kuipers, T.M. Klapwijk, G. Borghs, Phys. Rev. B **57**, 11911 (1998).
- [56] C.-M. Hu, J. Nitta, T. Akazaki, H. Takayanagi, J. Osaka, P. Pfeffer, and W. Zawadski, Phys. Rev. B **60**, 7736 (1999).
- [57] G. Salis, Y. Kato, K. Ensslin, D.C. Driscoll, A.C. Gossard, and D.D. Awschalom, Nature **414**, 619 (2001).
- [58] J. H. Smet, R. A. Deutschmann, F. Ertl, W. Wegscheider, G. Abstreiter, K. von Klitzing, Nature **415**, 281 (2002).
- [59] F.T. Vas'ko, and N.A. Prima, Fiz. Tverd. Tela **21**, 1734 (1979) [Sov. Phys. Solid State **21**, 994 (1979)].
- [60] U. Rössler, Solid State Comm. **49**, 943 (1984).
- [61] M. Cardona, N.E. Christensen, G. Fasol, Phys. Rev. B **38**, 1806 (1988).
- [62] G. Lommer, F. Malcher, U. Rössler, Phys. Rev. Lett. **60**, 728 (1988).
- [63] J. Luo, H. Munekata, F.F. Fang, and P.J. Stiles, Phys. Rev. B **38**, 10142 (1988).
- [64] B. Das, D.C. Miller, S. Datta, R. Reifenberger, W.P. Hong, P.K. Bhattacharya, J. Singh, M. Jaffe, Phys. Rev. B **39**, 1411 (1989).
- [65] J. Luo, H. Munekata, F.F. Fang, and P.J. Stiles, Phys. Rev. B **41**, 7685 (1990).
- [66] Yu.L. Ivanov, P.S. Kop'ev, S.D. Suchalkin, and V.M. Ustinov, Pis'ma ZhETP **53**, 470 (1991) [Sov. JETP Lett. **53**, 493 (1991)]
- [67] P.D. Dresselhaus, C.M. A. Papavassiliou, R.G. Wheeler, R.N. Sacks, Phys. Rev. Lett. **68**, 106 (1992).
- [68] E.A. de Andrada e Silva, Phys. Rev. B **46**, 1921 (1992).
- [69] R.V. Santos, and M. Cardona, Phys. Rev. B **72**, 432 (1994).??
- [70] E.A. Andrada e Silva, G.C. La Rocca, and F. Bassani, Phys. Rev. B **50**, 8523 (1994).
- [71] B. Jusserand, D. Richards, G. Allan, C. Priester, and B. Etienne, Phys. Rev. B **51**, 4707 (1995).
- [72] P. Pfeffer, and W. Zawadski, Phys. Rev. B **52**, R14332 (1995).
- [73] E.L. Ivchenko, A.Yu. Kaminski, and U. Rössler, Phys. Rev. B **54**, 5852 (1996).
- [74] G. Engels, J. Lange, Th. Schäpers, and H. Lüth, Phys. Rev. B **55**, R1958 (1997).

- [75] E.A. Andrada e Silva, G.C. La Rocca, and F. Bassani, Phys. Rev. B **55**, 16293 (1997).
- [76] D. Grundler, Phys. Rev. Lett. **84**, 6074 (2000).
- [77] P.R. Hammar, M. Johnson, Phys. Rev. B **61**, 7207 (2000).
- [78] J.A. Majewski, P. Vogl, P. Lugli, Proc. of the 25th Int. Conf. of Physics of Semiconductors (ICPS), Eds. N. Miura, T. Ando, Springer Verlag Berlin, 791 (2001).
- [79] Z. Wilamowski, W. Jantsch, H. Malissa, and U. Rössler, Phys. Rev. B **66**, 195315 (2002).
- [80] S.A. Tarasenko, and N.S. Averkiev, Pis'ma ZhETF **75**, 669 (2002) [Sov. JETP Lett. **75**, 552 (2002)].
- [81] O. Krebs, and P. Voisin, Phys. Rev. Lett. **77**, 1829 (1996).
- [82] T. Guettler, A.L.C. Triques, L. Vervoort, R. Ferreira, Ph. Roussignol, P. Voisin, D. Rondi, and J.C. Harmand, Phys. Rev. B **58**, R10179 (1998).
- [83] O. Krebs, D. Rondi, J.L. Gentner, L. Goldstein, and P. Voisin, Phys. Rev. Lett. **80**, 5770 (1998).
- [84] A.A. Toropov, E. L.Ivchenko, O. Krebs, S. Cortez, P. Voisin, and J.L. Gentner, Phys. Rev. B **63**, 035302 (2000).
- [85] J.T. Olesberg, W.H. Lau, M. Flatte, C.Yu.E. Altunkaya, E.M. Shaw, T.C. Hasenberg, and T. Bogges, Phys. Rev. B **64**, 201301 (2001).
- [86] U. Rössler, and J. Kainz, Solid State Comm. **121**, 313 (2002).
- [87] L.E. Golub, and E.L. Ivchenko, to be published (cond-mat/0302308).
- [88] G. Dresselhaus, Phys. Rev. **100**, 580 (1955).
- [89] E.I. Rashba, Fiz. Tverd. Tela **2** 1224 (1960) [Sov Phys. Sol. State **2**, 1109 (1960)].
- [90] S. Datta, B. Das, Appl. Phys. Lett. **56**, 665 (1990).
- [91] E.L. Ivchenko, and S.A. Tarasenko, JETP, to be published.
- [92] A. Haché, Y. Kostoulas, R. Atanasov, J.L.P. Hudges, J.E. Sipe, and H.M. van Driel, Phys. Rev. Lett. **78**, 306 (1997).
- [93] A.G. Aronov, and Yu. B. Lyanda-Geller, Pis'ma ZhETP **50**, 398 (1989) [Sov. JETP Lett. **50**, 431 (1990)].
- [94] V.M. Edelstein, Solid State Comm. **73**, 233 (1990).
- [95] R.R. Parson, Can. J. Phys. **49**, 1850 (1971).
- [96] W. Hanle, Zeitschrift für Physik **30**, 93 (1924).
- [97] A.V. Andrianov, and I.D. Yaroshetskii, Pis'ma ZhETF **40**, 131 (1984) [Sov. JETP Lett. **40**, 882 (1984)].
- [98] E.L. Ivchenko, Yu.B. Lyanda-Geller, and G.E. Pikus, Solid State Commun. **69**, 663 (1989).
- [99] M. Behet, S. Nemeth, J. DeBoeck, G. Borghs, J. Tümmeler, J. Woitok, J. Geurts Semicond. Sci. Techn. **13**, 428 (1998).
- [100] R. Fiederling M. Keim, G. Reuscher, W. Ossau, G. Schmidt, A. Waag, and L.W. Molenkamp, Nature **402**, 787 (1999).
- [101] S.D. Ganichev, Physica B **273-274**, 737 (1999).

[102] S.D. Ganichev, I.N. Yassievich, and W. Prettl, *J. Phys.: Condens. Matter* **14**, R1263 (2002).

[103] G.M.H. Knippels, X. Yan, A.M. MacLeod, W.A. Gillespie, M. Yasumoto, D. Oepts and A.F.G. van der Meer, *Phys. Rev. Lett.* **83**, 1578 (1999).

[104] S.D. Ganichev, Ya.V. Terent'ev, and I.D. Yaroshetskii, *Pis'ma Zh. Tekh. Phys.* **11**, 46 (1985) *Sov. Tech. Phys. Lett.* **11**, 20 (1985).

[105] E.V. Beregulin, S.D. Ganichev, I.D. Yaroshetskii, P.T. Lang, W. Schatz, and K.F. Renk, *Proc. SPIE* **1362-2**, ed by M. Razeghi, 853 (1990).

[106] R.J. Warburton, C. Gauer, A. Wixforth, and J.P. Kotthaus, B. Brar, and H. Kroemer, *Phys. Rev. B* **53**, 7903 (1996).

[107] V.V. Bel'kov, S.D. Ganichev, Petra Schneider, D. Schowalter, U. Rössler, W. Prettl, E.L. Ivchenko, R. Neumann, K. Brunner, and G. Abstreiter, *J. of Supercond.: Incorporating Novel Magn.* **16**, 419 (2003) (cond-mat/0301389).

[108] X. Marie, T. Amand, P. Le Jeune, M. Paillard, P. Renucci, L.E. Golub, V.D. Dymnikov, and E.L. Ivchenko, *Phys. Rev. B* **60**, 5811 (1999).

[109] G. Lampel, *Phys. Rev. Lett.* **20**, 491 (1968).

[110] A.I. Ekimov, and V.I. Safarov, *Pis'ma ZhETF* **12**, 293 (1970) [Sov. JETP Lett. **12**, 198 (1970)].

[111] B.I. Zakharchenya, V.G. Fleisher, R.I. Dzhioev, Yu.P. Veshchunov, and I.B. Rusanov, *Pis'ma ZhETF* **13**, 195 (1971) [Sov. JETP Lett. **13**, 137 (1971)].

[112] A.M. Danishevskii, E.L. Ivchenko, S.F. Kochegarov, and V.K. Subashiev, *Fiz. Tverd. Tela* **27**, 710 (1985) [Sov. Phys. Solid State **27**, 439 (1985)].

[113] R. Ferreira, and G. Bastard, *Phys. Rev. B* **43**, 9687 (1991).

[114] L.E. Vorobjev, D.V. Donetskii, and L.E. Golub, *Pis'ma ZhETF* **63**, 977 (1996) [Sov. JETP Lett. **63**, 981 (1996)].

[115] Petra Schneider, S.D. Ganichev, J. Kainz, U. Rössler, W. Wegscheider, D. Weiss, W. Prettl, V.V. Bel'kov, L.E. Golub, D. Schuh, *phys.stat. sol. a*, to be published (cond-mat/0303056).

[116] J. Shah, *Ultrafast spectroscopy of semiconductor nanostructures*, Springer (1999), pp. 243-261.

[117] L. Viña, *J. Phys.: Condens. Matter* **11**, 5929 (1999).

[118] I.D. Yaroshetskii, and S.M. Ryvkin, in *Problems of Modern Physics* (in Russian), ed. V.M. Tuchkevich and V.Ya. Frenkel, Leningrad, Nauka, 1980, p.173 [English translation: *Semiconductor Physics*, ed. V.M. Tuchkevich and V.Ya. Frenkel, Cons. Bureau, New York, 1986, p. 249].

[119] A.F. Gibson, and M.F. Kimmitt *Photon Drag Detection* in: *Infrared and Millimeter Waves*, ed. by K.J. Button, N.Y., **3**, 182 (1980).

[120] A.M. Glass, D. von der Linde, and T.J. Negran, *Appl. Phys. Lett.* **25**, 233 (1974).

[121] V.I. Belinicher, V.K. Malinovskii, and B.I. Sturman, *ZhETF* **73**, 692 (1977) [Sov. JETP Lett. **46**, 362 (1977)].

[122] L.I. Magarill, and M.V. Entin, *Poverchnost'* **1**, 74 (1982) [Sov. Surface **1**, 74 (1982)].

[123] G.M. Gusev, Z.D. Kvon, L.I. Magarill, A.M. Palkin, V.I. Sozinov, O.A. Shegai, and M.V. Entin, *Pis'ma ZhETP* **46**, 28 (1987) [Sov. JETP Lett. **46**, 33 (1987)].

[124] H. Schneider, S. Ehret, C. Schönbein, K. Schwarz, G. Bihlmann, J. Fleissner, G. Tränkle, and G. Böhm, *Superlatt. Microstruct.* **23**, 1289 (1998).

[125] R. von Baltz and W. Kraut, *Phys. Lett. A* **79**, 364 (1980).

[126] V.I. Belinicher, E.L. Ivchenko, and B.I. Sturman, *ZhETF* **83**, 649 (1982) [Sov. JETP **56**, 359 (1982)].

[127] E.L. Ivchenko, Yu.B. Lyanda-Geller, and G.E. Pikus, *Fiz. Tekh. Poluprov.* **18**, 93 (1984) [Sov. Phys. Semicond. **18**, 55 (1984)].

[128] A.V. Andrianov, E.V. Beregulin, S.D. Ganichev, K.Yu. Gloukh, and I.D. Yaroshetskii, *Pis'ma Zh. Tekh. Fiz.* **14**, 1326 (1988) Sov. Tech. Phys. Lett. **14**, 580 (1988).

[129] C. Schönbein, H. Schneider, G. Bihlmann, K. Schwarz, and P. Koidl, *Appl. Phys. Lett.* **68**, 973 (1995).

[130] A.M. Danishevskii, A.A. Kastal'skii, S.M. Ryvkin, and I.D. Yaroshetskii, *ZhETF* **58**, 544 (1970) [Sov. JETP **31**, 292 (1970)].

[131] A.F. Gibson, M.F. Kimmit, and A.C. Walker, *Appl. Phys. Lett.* **17**, 75 (1970).

[132] S. Luryi, *Phys. Rev. Lett.* **58**, 2263 (1987).

[133] A.D. Wieck, H. Sigg, and K. Ploog, *Phys. Rev. Lett.* **64**, 463 (1990).

[134] A.A. Grinberg and S. Luryi, *Phys. Rev. B* **38**, 87 (1988).

[135] A.P. Dmitriev, S.A. Emel'yanov, S.V. Ivanov, P.S. Kop'ev, Ya.V. Terent'ev, and I.D. Yaroshetskii, *Pis'ma ZhETF* **54**, 460 (1991) [Sov. JETP Lett. **54**, 462 (1991)].

[136] O. Keller, *Phys. Rev. B* **48**, 4786 (1993).

[137] E.V. Beregulin, P.M. Voronov, S.V. Ivanov, P.S. Kop'ev, and I.D. Yaroshetskii, *Pis'ma ZhETF* **59**, 83 (1994) [Sov. JETP Lett. **59**, 85 (1994)].

[138] F.T. Vasko, *Phys. Rev. B* **53**, 9576 (1996).

[139] F.T. Vasko, and O. Keller, *Phys. Rev. B* **58**, 15666 (1998).

[140] H. Sigg, M.H. Kwakermaak, B. Margotte, D. Erni, P. van Son, and K. Köhler, *Appl. Phys. Lett.* **67**, 2827 (1995).

[141] I. Žutić, J. Fabian, and S. Das Sarma, *Appl. Phys. Lett.* **79**, 1558 (2001).

[142] I. Žutić, J. Fabian, and S. Das Sarma, *Phys. Rev. Lett.* **88**, 066603 (2002).

[143] E.L. Ivchenko, B. Spivak, *Phys. Rev. B* **66**, 155404 (2002).